# THEORETICAL STUDY OF PHOTOEMISSION FROM METALS AND SEMICONDUCTORS

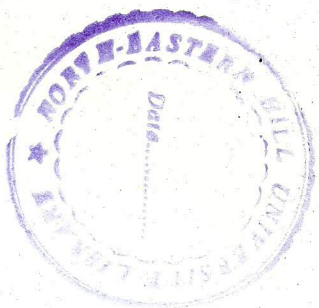


By
Zaithanzauva Pachuau
Department of Physics

Submitted
in partial fulfillment of the requirement of the
Degree of Doctor of Philosophy in Physics of
North Eastern Hill University, Shillong

# THEORETICAL STUDY OF PHOTOEMISSION FROM METALS AND SEMICONDUCTORS


## ABSTRACT

# CHAPTER 1

# INTRODUCTION



Photoemission is basically concerned with the emission of electrons from the surface/bulk of metals by the incident electromagnetic radiation in the ultra-violet (UV) region. Photoemission spectroscopy has now been widely used as a method for studying the electronic properties of solids. But the detailed interpretation of the photoemission data requires the use of a theory of photoemission which should in its simplest form be able to calculate the initial and final state electronic wave functions, as well as the spatial form of the vector potential which is involved in photoemission matrix element i.e. $< \psi_f |H'| \psi_i >$. Except Feibelman, very few authors have taken care to evaluate the initial state wave function $\psi_i$ involved in the formula for photocurrent in photoemission. However, the method of Feibelman could be extended only to free electron metals. In this thesis, we will be interested mainly in the formulation of initial state wavefunction by suitably choosing a model potential which would be equally applicable to free electron metals, d-band metals as well as semiconductors. This would enable one to interpret the measured photocurrent data in a more realistic approach.

Electronic properties of solids are found to be different in the surface region than in the bulk region. The reason for this being that the presence of surface modifies the electronic properties due to loss of the periodicity in the direction normal to the surface. The electronic distribution may differ quite significantly from that in the

bulk, although the region important for this departure from bulk value is only a few lattice parameters. There may be new types of states, surface states or resonances which are spatially located in the surface region, and the case of pure surface states are forbidden in the bulk. Experimental techniques like angle-resolved photoemission, field-emissions, photo-field emissions, inverse photoemissions etc. can well be used to probe these states in the surface region. However, while angle-resolved photoemissions can also be used to study these states, the variations of the electromagnetic fields associated with photon in the surface presents an additional problem. Due to complex problem created by the presence of the surface in photoemission studies, many authors have neglected the effect of the variation of the electromagnetic fields with photon energy.

As *ab initio* treatment of the variation of fields near surfaces is extremely a complex situation involving tremendously a large computational effort, we will be using simple dielectric model to compute these fields. The dielectric model in which the dielectric function is assumed to vary linearly as a function of the distance from the surface region, can be solved to get the electromagnetic fields in the region of interest. The important thing with this model being that the dielectric function is a function of both frequency and spatial co-ordinate. The dielectric function interpolates linearly between the bulk value inside the metal and the vacuum value (unity) outside. In this model, the complex dielectric constant of metals is evaluated by using the experimentally determined frequency-dependent dielectric functions. We have used this model or its modified form for calculations of electromagnetic fields in the

metals and semiconductors. The fields so determined will be used for calculating the photoemission cross-sections for determining the photocurrent as a function of photon energy by evaluating the matrix element $< \psi_f |H'| \psi_i >$. The behaviour of photocurrent especially near the plasmon energy of metals under study would be of particular interest.

The exact formulation of the initial state wavefunction by choosing the appropriate potential model for the surface and the bulk regions of the solid is very important and complex too in photoemission study. There are various approaches to surface and bulk photoemission calculations which had been applied to real cases. In this proposal, we are considering as a first step, the applications of Kronig-Penney(KP) model potential as applied by Thapa and others to metals and semiconductors. We have formulated the initial state wavefunction $\psi_i$ in such a way that it takes into account both the surface and the bulk potential using the Mathieu potential model. A realistic type of calculations for the surface state in photoemission has been done by Levine using this model which was proposed at first by Statz. In this type of potential given by $V = V_o \cos(\frac{2\pi x}{a})$, the amplitude $V_o$ is a measure of the crystal potential strength in a mono-atomic crystal, and the ionicity in a di- atomic one. When $V_o$ is small (large), the Mathieu potential model approaches the Nearly Free Electron(Tight Binding Approximation) limit, and thus acts as a bridge between these two extreme conditions. Davison and Levine, Slater and Carver have used the Mathieu potential to describe the energy bands in a realistic crystal. We, therefore, find that no such calculations have been done in photoemission which incorporates both the

photon field variation and the initial state derived by using the Mathieu potential model. This potential would be used to solve Schroedinger's equation, the wavefunction and its derivative being evaluated at z = 0 plane. The formulated $\psi_i$ would be then used to calculate the photocurrent from metals and semiconductors. The final state wavefunction $\psi_f$ will be the scattering final state of the step like potential existing at the surface defined by $V(z) = -V_o\theta(z)$, which an electron encounters when it is being transmitted through the surface. The Golden Rule formula for calculating the photocurrent density is given by

$$\frac{dj}{d\omega} = \frac{2\pi}{\hbar} \Sigma | < \psi_f | H' | \psi_i > |^2 \delta(E - E_f)\delta(E_f - E_i - \hbar\omega)\, f_o(E - \hbar\omega)\,[1 - f_o(E)] \qquad (1.1)$$

where $H'$ is the perturbation responsible for photoemission by radiation of frequency, $|\psi_i>$ and $|\psi_f>$ refers to the initial(final) state wavefunction, $E_i(E_f)$ refers to the initial(final) state energy, $f_o(E)$ denotes the Fermi occupation function. We are considering the photoemission to take place along z-axis which is normal to the surface. We may therefore write $H'$ as

$$H' = \frac{e}{mc}[\tilde{A}_\omega(z)\frac{d}{dz} + \frac{1}{2}\frac{d}{dz}\tilde{A}_\omega(z)] \qquad (1.2)$$

where $\tilde{A}_\omega(z) = \frac{A^z_\omega(z)}{A_o}$ with $A^z_\omega(z)$ as the component of vector potential along z-axis, $A_o$ is the amplitude of the incident beam. The formula for photoemision cross-section can be written as

$$\frac{d\sigma}{d\Omega} \approx \frac{k^2}{\omega} | < \psi_f | \tilde{A}_\omega(z)\frac{d}{dz} + \frac{1}{2}\frac{d}{dz}\tilde{A}_\omega(z) | \psi_i > |^2 \qquad (1.3)$$

In this thesis, we have developed a simple formalism for photoemission calculation in which the free electron states are derived by using the Mathieu potential. The Mathieu potential has been at first used by Statz for surface state calculation. Levine had also used Mathieu potential for calculating the condition for arbitrary surface termination. We have used in this formalism the model as described by Davison and Steslicka for describing the crystal potential which was then used for deriving the initial state wavefunction for photocurrent calculations.

To compute the photon field, we have used the simple model of Bagchi and Kar which has been used earlier also. To determine the inital state wavefunction $\psi_i$ , we have considered, at first an empty lattice with a finite step potential. The photocurrent was calculated as a function of photon energy ($\hbar\omega$). The formalism was then applied to the case of free electron metals like aluminium and berylium. For these metals, we have used the experimentally determined dielectric function for calculating the photocurrent through the subroutine of the main FORTRAN program. We find that in the case of Al and Be, there is a qualitative agreement between the theoretical and experimental data. We then extend this model for a finite surface potential with strong periodic lattice and apply it to solids like tungsten, molybdenum and semiconductor silicon. Using the initial state wavefunction derived with this model, we used the field obtained from the experimental data of dielectric functions and discuss the photocurrent calculations.

The topics in this thesis are arranged as follows : In Chapter 2, we shall discuss the model of dielectric response function used for the calculation of the electromagnetic field (photon field vector) for the vacuum, surface and bulk region of the solids. This photon field vector was then used to calculate the field for solids like

beryllium, molybdenum, tungsten and silicon. In Chapter 3, photoemission calculations using the Kronig-Penney model will be discussed. The dielectric model of Bagchi and Kar and also Lorentz-Drude dielectric model will be used to calculate the field which were then applied to calculate the photocurrent in the case of metals like molybdenum, copper, tungsten and semiconductors silicon and gallium arsenide. The relativistic effect in the band state calculation of photoemission is also briefly discussed in Chapter 3. In Chapter 4, we shall discuss the formulation of the initial state wavefunction by using the Mathieu potential model and discuss a number of applications.

# CHAPTER 2

## DIELECTRIC MODEL AND ELECTROMAGNETIC FIELD

In this chapter, we shall discuss the dielectric model used and the calculation of electromagnetic field in a solid when electromagnetic radiation is incident on it. The calculation of the fields near a surface is a complex problem and *ab initio* calculations have been done only for jellium. However, these calculations have not been exentended to other metals where the jellium model is not applicable. Further, if one wants to consider the field variation in the presence of surface for metals, e.g. d-band metals like tungsten, molybdenum, palladium,etc., one has to use simpler models. The dielectric model used by Bagchi and Kar for the case of tungsten has been used for the calculation of the electromagnetic field in the surface region. This model involves the linear interpolation in the surface region between the bulk dielectric function and the vacuum value. Though it has some deficiencies, it is important to note that it is a local response function and can be traced as shown by the application to tungsten and aluminium. It also gives good results in agreement with the experimentally determined value. Since the bulk dielectric value required for this model is obtained experimentally, the field calculation can be extended to the case of semiconductors. We will briefly describe the dielectric model used and the calculation of the electromagnetic fields from it.

### 2.1 Calculation of Dielectric Model and Electromagnetic Field :

The dielectric model used is the one given by Bagchi and Kar which is shown in Fig. (2.1). The metal is assumed to occupy the space to the left of the z-plane. In the region $-a \leq z \leq 0$ , the dielectric constant is chosen to be a local function which

interpolates linearly between the bulk value inside the metal and the vacuum value(unity) outside. The model frequency-dependent dielectric function is, therefore, given by

$$\varepsilon(\omega,z)=\begin{cases}\varepsilon_1(\omega)+i\varepsilon_2(\omega), & \text{for} \quad z<-a\\ 1+[1-\varepsilon(\omega)]\frac{z}{a} & \text{for} \quad -a\le z\le 0\\ 1, & \text{for} \quad z>0.\end{cases} \tag{2.1}$$

The incident radiation is taken to be p-polarised of frequency $\omega$ and incident on the surface at an angle of incidence $\theta_i$ . A gauge was chosen in which the scalar potential **A** is set equal to zero and the electromagnetic field $E(Q,\omega,z)$ is expressed in terms of the vector potential as

$$E(Q,\omega,z)=\frac{i\omega}{c}A(Q,\omega,z) \tag{2.2}$$

where $Q=\frac{\omega}{c}\sin\theta_i$. The magnetic field B(z)= $A(Q,\omega,z)$ points in the y-direction and it follows that :

$$\frac{d}{dz}\left(\frac{1}{\varepsilon}\frac{dB}{dz}\right)+\left(\frac{\omega^2}{c^2}-\frac{Q^2}{\varepsilon}\right)B=0, \tag{2.3}$$

where $\varepsilon=\varepsilon(\omega,z)$. The electric field component can be obtained from the magnetic field as

$$E^x(Q,\omega,z)=\frac{c}{i\omega\varepsilon}\frac{dB}{dz}$$
$$E^z(Q,\omega,z)=-\frac{\sin\theta_i}{\varepsilon}B \tag{2.4}$$

To solve Eq. (2.3), a new variable u(z) was introduced according to the discussion of Landau and Lifshitz which is given by $B(z) = u(z)\sqrt{\varepsilon}$. Then u(z) satisfies the equation :

$$\frac{d^2u}{dz^2} + \frac{\omega^2}{c^2}(\varepsilon - \sin^2\theta_i)\,u + [\frac{1}{2\varepsilon}\frac{d^2\varepsilon}{dz^2} - \frac{3}{4}\frac{1}{\varepsilon^2}(\frac{d\varepsilon}{dz})^2]\,u = 0 \qquad (2.5)$$

For the dielectric model used, $\frac{d\varepsilon}{dz}$ is finite only in the region $-a \le z \le 0$ and $\frac{d^2\varepsilon}{dz^2}$ vanishes everywhere except for singularities at $z = \pm a$. The vector potential $\tilde{A}_\omega(z) = \frac{E^z_\omega(z)}{E_o}$ in the long wavelength limit $(\omega\frac{a}{c}) \to 0$ is then given by :

$$\tilde{A}_\omega(z) = \begin{cases} -\dfrac{\sin 2\theta_i}{[\varepsilon(\omega)-\sin^2\theta_i]^{\frac{1}{2}}+\varepsilon(\omega)\cos\theta_i} & z < -a \\ -\dfrac{\sin 2\theta_i}{[\varepsilon(\omega)-\sin^2\theta_i]^{\frac{1}{2}}+\varepsilon(\omega)\cos\theta_i}\cdot\dfrac{a\varepsilon(\omega)}{[1-\varepsilon(\omega)]z+a} & -a \le z \le 0 \\ -\dfrac{\varepsilon(\omega)\sin 2\theta_i}{[\varepsilon(\omega)-\sin^2\theta_i]^{\frac{1}{2}}+\varepsilon(\omega)\cos\theta_i} & z > 0. \end{cases} \qquad (2.6)$$

The electromagnetic fields have been calculated for photon energy below and above the plasmon energy of the metals and semiconductors. The electromagnetic fields have been for beryllium, molybdenum, tungsten and silicon. We have plotted $|\tilde{A}_\omega(z)|$ as a function of photon energy ( $\hbar\omega$ ) and the distance (z) from the surface of the solids and the results are discussed.

# CHAPTER 3

# PHOTOCURRENT CALCULATIONS USING KRONIG-PENNEY MODEL

We have used the Kronig-Penney model potential to find the initial state wavefunction. The initial state wavefunction $\psi_i$ was formulated by the method of normal matching of the wavefunctions at the boundary surface of the solid. The photocurrent was then calculated by using the electromagnetic fields developed by Bagchi and Kar. The free electron(FE) model has been successful in explaining the photoemission phenomena from free electron metals. But it has drawback in explaining the band structure effects of solid. Kronig-Penney(K-P) model has then been used for the calculations of surface electronic states by several authors. Schaich and Ashcroft have calculated numerically the photoyield by using the modified form of the Kronig-Penney model. Steslicka had done a detailed calculations of the surface states using the Kronig-Penney model both for the semi-infinite and infinite crystals. Eldib *et. al.* has also applied the Kronig-Penney model to one dimensional crystal.

## 3.1 **Kronig-Penney potential model** :

In this section, we shall discuss the Kronig-Penney(K-P) model as developed by Thapa *et. al.* for the calculation of photocurrent from metals and semiconductors. The Kronig-Penney model was used to represent the crystal potential field by a linear array of rectangular well (Fig. 3.1), which was later transformed into a chain of $\delta$-function potential well such that the area of each well remains constant. The initial state wavefunction was obtained by matching at the surface.

To evaluate the initial state wavefunction $\psi_i(z)$, one can solve the one-dimensional Schroedinger's equation given by :

$$\frac{d^2\psi(z)}{dz^2} + k_i^2(z) = -2V(z)\psi(z), \tag{3.1}$$

where $k_i^2 = 2E_i$ and $V(z)$ is the $\delta$–function potential of the K-P model.

Let $\phi(z)$ denote the Bloch wavefunction deep inside the metal and $\phi^*(z)$ the time reversal of $\phi(z)$. The eigenfuction in the semi-infinite solid $(z < 0)$ was chosen to have the form as :

$$\psi_i(z) = \phi(z) - P\phi^*(z) \tag{3.2}$$

where $P$ is the reflection coefficient obtained by matching the wavefunction and its derivative at $z = 0$. The potential $V(z)$ was considered to be one-dimensional Kronig-Penney type given by :

$$V(z) = = \Sigma\, g\ \delta[z - (2n+1)\tfrac{d}{2}] \tag{3.3}$$

One can then show that the initial state wavefunction for the bulk, surface and vacuum regions may be written as

$$\psi_i = \begin{cases} (1 - iPe^{-i\delta}\sin\delta)e^{ik_i z} - (P - ie^{i\delta}\sin\delta)e^{-ik_i z}, & z \le 0 \\ \text{(bulk \& surface)} & \\ Te^{-\kappa z}, & z < 0 \text{ (vacuum)} \end{cases} \tag{3.4}$$

where $\cot\delta = -\frac{k_i}{g}$, $\delta$ is the phase shift introduced in the transmitted wave, $g$ is the strength of the $\delta$ - potential which describes the bulk potential, $T$ being the transmission coefficient across the boundary plane and $\kappa^2 = 2(V_o - E_i)$, where $V_o$ is the potential at the surface which an electron encounters while transmitting through the boundary surface. From the matching conditions at z = 0, one can easily deduce the values of $P$ and $T$ in Eq. (3.4) which is given by :

$$P = \frac{(\kappa - ik_i) - (k_i - i\kappa)e^{i\delta}\sin\delta}{(\kappa - ik_i) - (k_i - i\kappa)e^{-i\delta}\sin\delta} \tag{3.5}$$

and

$$T = \frac{2k_i \sin 2\delta}{(\kappa - ik_i) + (k_i - i\kappa)e^{-i\delta}\sin\delta} \tag{3.6}$$

The proper evaluation of $P$ and $T$ with the correct numerical values for other factors enables one to write the most explicit form of initial state wavefunction $|\psi_i>$. The photo emission cross-section was obtained by using the formula

$$\frac{d\sigma}{d\Omega} = \frac{k^2}{\omega}\Sigma |<\psi_f|H'|\psi_i>|^2 \tag{3.7}$$

The matrix element given in Eq. (3.7) can be written as

$$I = \int_{-\infty}^{-d} \psi_f^* \tilde{A}_\omega(z)\frac{d\psi_i}{dz}dz + \int_{-d}^{0} \psi_f^* \tilde{A}_\omega \frac{d\psi_i}{dz}dz$$

$$+\frac{1}{2}\int_{-d}^{0} \psi_f^* \frac{d\tilde{A}_\omega}{dz}\psi_i dz + \int_0^\infty \psi_f^* \tilde{A}_\omega(z)\frac{d\psi_i}{dz}dz. \tag{3.8}$$

In Eq. (3.8), the final state wavefunction $\psi_f(z)$ is the scattering state of the step potential V(z) given by $V(z) = -V_o\theta(z)$. Here $V_o = E_F + \phi$, where $E_F$ is the Fermi level and $\phi$ is the work function. The final state wavefunction can be written as (in atomic units) :

$$\psi_f(z) = \begin{cases} \left(\frac{1}{2\pi q_f}\right)^{\frac{1}{2}} \frac{2q_f}{q_f+k_f} e^{ik_f z} e^{-\alpha|z|}, & z \le 0 \text{ (bulk \& surface)} \\ \left(\frac{1}{2\pi q_f}\right)^{\frac{1}{2}} \left[e^{iq_f z} + \left(\frac{q_f-k_f}{q_f+k_f}\right) e^{-iq_f z}\right], & z > 0 \text{ (vacuum)} \end{cases} \quad (3.9)$$

where $k_f^2 = 2E_f$, $q_f^2 = 2(E_f - V_o)$ and $E_f = E_i + \hbar\omega$. In Eq. (3.9), the factor $e^{-\alpha|z|}$ ($\alpha$ is the scattering factor) is included on the surface and bulk side to take into account the inelastic scattering of the electrons. The photocurrent was calculated numerically by evaluating (3.8). The FORTRAN program used is given in Appendix- E. In our calculations, we have used the respective dielectric functions corresponding to different solids as given by Weaver and Edwards. The solids which we have used are molybdenum, copper, tungsten and silicon.

## 3.2 **Kronig-Penney model calculations using Lorentz-Drude dielectric model** :

In this section, we show the behaviour of photocurrent calculated by using the Lorentz-Drude model for the dielectric constant in the case of semiconductors. As discussed in the previous chapter, the existence of surface states on semiconductor surfaces was experimentally verified by using the angle integrated photoemission. The semiconductor surfaces are more complex than metal surfaces for the reason that semiconductor surfaces reconstruct. The presence of these reconstructed ions and atomic displacements on semiconductor surfaces makes the studies of electronic structure a

very interesting topic. Of the various tools and techniques, angle resolved photoemission studies has also been widely used in understanding the surface states of semiconductors. But in this section, we will be mainly concerned with the photoemission studies by adopting a simple procedure which will be applied to the case of silicon and gallium arsenide.

The Drude-Lorentz model for calculating the frequency dependent dielectric constants which is given by :

$$\varepsilon(\omega) = \varepsilon_\infty[1 - \frac{\omega_p^2}{\omega(\omega+i\gamma_1)}] + \frac{(\varepsilon_o-\varepsilon_\infty)\omega_0^2}{(\omega_0^2-\omega^2-i\gamma_2\omega)} \qquad (3.10)$$

In Eq. (3.10) above, $\varepsilon_o$ and $\varepsilon_\infty$ are the static and high frequency dielectric constants. By using the appropriate values of constants $\varepsilon_o$, $\varepsilon_\infty$, $\gamma_1, \gamma_2$ etc. respectively for silicon and gallium arsenide, the real and imaginary parts of $\varepsilon(\omega)$ were calculated. Using the electromagnetic fields for p-polarized radiation, we calculate the photoemission cross-section by evaluating the matrix element in Eq. (3.9). and applied to the case of silicon and gallium arsenide. In our calculations though we have not taken into consideration the effect of type of semiconductor, density, etc., we find that the spatial dependence of vector potential is an essential ingredient in photoemission calculations. It would be more realistic if one can employ the method as developed by Cappellini *et. al.* which is specifically defined only for the semiconductors. Further, the inclusion of crystal structure into this type of calculations will enable one to compare the data with experiment in a more realistic way. For example, a detailed study of photoemission from gallium arsenide by using the one-step model of photoemission had been done by Schattke. The photoemission data for the ideal gallium arsenide surface agreed well with the experimental data.

## 3.3 Relativistic Kronig-Penney potential model calculation of photoemission :

In the above treatments of photoemission calculations both in the case of metals and seminconductors, the spin of the electrons in the formulations of the initial state wavefunctions were not taken into considerations. This implied that the relativistic effects were omitted and it was purely a non-relativistic type of calculations. We have considered in the same way the variations of the dielectric functions for the calculations of the photon fields but adopted the wavefunctions for the initial state of the electrons as developed by Davison and Steslicka. We have introduced the surface of width '*d*' into the potential model and used the wavefunctions for the evaluation of the matrix elements for photocurrent calculations. The model was applied to the case of heavy atomic solids like tungsten and silicon.

The crystal potential model as used by DS for deriving $\psi_i$ has a surface width $d$. The crystal potential is given by $LtV_3 b = a_o$ with $b$ as the width of

$$V_3 \to 0$$

$$b \to 0$$

the potential barrier and (a+b) the period of the potential, $a_o$ being a positive quantity. On solving the one-dimensional time-independent Dirac equation, we get :

$$i\hbar c\frac{d\phi_k^{(1)}}{dx} = (\varepsilon_o - V_k)\phi_k^{(2)} \tag{3.11}$$

and

$$i\hbar c\frac{d\phi_k^{(2)}}{dx} = \{(\varepsilon_o - V_k) + 2m_o c^2\}\phi_k^{(1)} \tag{3.12}$$

Decoupling Eqs. (3.11) and (3.12) leads to

$$i\hbar c\frac{d\phi_k^{(j)}}{dx} = -\rho_k^2\phi_k^{(j)}, \qquad j = 1,2 \qquad (3.13)$$

where wave vector $\rho_k^2 = (\varepsilon_o - V_k)[(\varepsilon_o - V_k) + 2m_oc^2]/\hbar^2c^2$.

The plane wave solution of Eq. (3.13) for bulk (x>0) and vacuum (x<0) regions can be written as :

$$\psi_i(x) = \phi_2(x) = a_2^{(2)}\left\{\begin{pmatrix} -\gamma_2 \\ 1 \end{pmatrix}e^{i\rho_2 x} + \lambda\begin{pmatrix} \gamma_2 \\ 1 \end{pmatrix}e^{-i\rho_2 x}\right\}, \qquad x > 0$$

$$\phi_1(x) = \begin{pmatrix} \gamma_1 \\ 1 \end{pmatrix}\beta_1^{(2)}e^{l_1 x}, \qquad x < 0 \qquad (3.14)$$

where $l_1 = -i\rho_1 > 0$ and is real. The constants in Eq. (3.14) are defined as

$$\varepsilon_o = \varepsilon - m_oc^2, \qquad a_k^{(1)} = -\gamma_k a_k^{(2)},$$

$$\beta_k^{(1)} = \gamma_k\beta_k^{(2)}, \qquad \gamma_k = \frac{\varepsilon_o - V_k}{\hbar c\rho_k}, \quad \text{and} \quad \lambda = \frac{\beta_2^{(2)}}{a_2^{(2)}} = \frac{1-e^{i(\rho_2-\mu)a}}{e^{-i(\rho_2+\mu)a}-1}.$$

$\mu$ is the wave number and is given by $\mu = \frac{n\pi}{a} + i\zeta$ where $\zeta$ is real and $\zeta > 0$.

The final state wavefunction $\psi_f$ which is correctly normalized in energy will be the scattering state of the step potential $V_1 = -V_o\theta(x)$, where $\theta(x)$ is a unit function. The vector potential $A$ is assumed to be a constant in the bulk and vacuum

regions but in the surface region, it is a function of x as the solution of Maxwell's equation for dielectric function $\in(x)$. The formula for the vector potential in one-dimension following Bagchi and Kar is given by

$$A_\omega(x) = \begin{cases} A_1, & x < 0 \text{ (bulk)} \\ \dfrac{A_1 \in(\omega) d}{[\in(\omega)-1]x+d}, & -d \leq x \leq 0 \text{ (surface)} \\ A_1 \in(\omega), & x > 0 \text{ (vacuum)} \end{cases} \qquad (3.15)$$

where $A_1$ is a constant depending on dielectric function $\in(\omega)$, photon energy $\hbar\omega$ and angle of incidence $\theta_i$.

We have calculated photocurrent against the incident photon energy ($\hbar\omega$) as a function of the band number ($n$) in the case of W and Si for $n$ = 2,4,6,8,10. The photoemission calculations in the case of W and Si using the non-relativistic Kronig-Penney(NR-KP) model have been done earlier. However, the behaviour of photocurent data in RKP case is completely different from that of NR-KP model.

The interesting feature which is seen in both the case of W and Si is that for the increase in band numbers the peak in photocurrent also goes on increasing. The only difference is that in the case of W, the highest peak on photocurrent is observed at $\hbar\omega - \hbar\omega_p$ (plasmon energy of tungsten which is 26 eV), whereas for Si it is obtained at photon energy 20 eV which is greater than its plasmon energy. This can be attributed to the fact that the band width $\Delta E_b$ goes on decreasing for the increase in band number. In other words, the relativistic correction reduces $\Delta E_b$ which causes the electrons to gain sufficient momenta due to rapid spatial variation of the incident radiation to be photoexcited. This causes the enhancement of photocurrent with the increase in $n$ in

both the cases of W and Si. In both the NR-KP and RKP treatment of photoemission, we find that only in the low frequency region photoemission is dominant due to spatial variation of the photon field vector. But the occurrence of peaks in photoemission by using the RKP model may be described as the manifestation of band structure effects in photoemission which has not been observed in the NR-KP cases. However, the occurrence of peaks in photocurrent data in the case of the relativistic treatment is attributed mainly due to inclusion of relativistic effects in photoemission.

The main drawback of including the initial state wavefunction $\psi_i$ as derived by DS is that it does not take into account the surface width. It has been well defined for both the vacuum and bulk regions. Further, we have not done any detailed calculations to derive the initial state wavefunction $\psi_i$. We also conclude from this study that the incorporation of the spatially variant vector potential is not sufficient. Further, the measured ultraviolet photoemission spectra(UPS) data have shown that effects due to spin-orbit coupling cannot be omitted in photoemissin spectra. Also the solution of Schrodinger's equation without the inclusion of spin-orbit interaction will become more and more inadequatein photoemission spectral measurements. One has to also modify the calculation for vector potential keeping in view the relativistic effects. There is, therefore, a need for relativistic theory of photoemission for accurate presentation of the UPS data.

# CHAPTER 4

## PHOTOCURRENT CALCULATIONS USING MATHIEU POTENTIAL MODEL

In the previous chapters, we have seen that photocurrent calculations was done by using various potential models in the case of metals and semiconductors. For example, free electron and Kronig-Penney potential models were used in the case of beryllium, tungsten, copper, silicon, etc. Photoemission studies were also carried out in the case of tungsten and silicon by using the relativistic Kronig-Penney model. We found that in the case of copper, Kronig-Penney model did not fit well since the plot did not show peak in photocurrent below the plasmon energy. With the increase of photon energy, the photocurrent also did not show a minimum at the plasmon energy. In the case of copper, maxima in photocurrent was measured at $\hbar\omega = 20$ eV with a minimum at $\hbar\omega = 26$ eV. Also, the application of relativistic Kronig-Penney model to W and Si showed too many peaks in photocurrent with the increase of photon energy. This is quite a different trend in the behaviour of photocurrent. These results do not conform to the calculated and measured data in photoemission when one is usually concerned with the variation of photocurrent against photon energy especially from the surface of metals. For this reason, we have applied Mathieu potential model to evaluate the initial state wavefunction to calculate the matrix element in photocurrent by using the same dielectric model as used in the earlier chapters. The photocurrent data obtained in this formalism could explain the behaviour of photocurrent also in the case of copper.

In this chapter, we shall use the Mathieu Potential model to represent the crystal potential. In this model, the potential is represented by a periodic sinusoidal wave in one-dimensional crystal. For such a potential, the Schrodinger equation reduces to the *Mathieu equation* whose solutions have been discussed in detail by McLachlan. The Mathieu potential had been used early by Brillouin and Morse. Brillouin had used this model as an appropriate model for developing the energy band theory of solids, while Morse used it in his study of electron diffraction. Slater used the Mathieu potential problem in one, two and three dimensions to describe the energy bands in a realistic crystal. Then Carver has discusssed the symmetries of Mathieu functions, and the relations between the functions and the electron wave functions at the centres and edges of the crystal bands. The Mathieu potential has been at first used by Statz for surface state calculation. Levine has used Mathieu potential for calculating the condition for arbitrary surface termination. In this chapter, we will discuss a formalism developed for photoemission calculations in which the electron states are derived by using the Mathieu potential. Two cases will be discussed namely, the effects of the empty lattice and strong periodic lattice potential on the electronic states for deriving the initial state wavefunctions as described by Davison and Steslicka.

## 4.1 **Empty Potential with Finite Surface :**

Let us consider a one-dimensional crystal whose potential is represented by a sinusoidal potential given by

$$V(x) = V_o \cos\left(\frac{2\pi x}{a}\right) \qquad (4.1)$$

where *'a'* is the period of the potential having a maximum value $V_o$ at x = 0.

The one-dimensional Schrodinger equation can be written as

$$\psi''(z) + (a - 2q\cos 2z)\psi(z) = 0 \qquad (4.2)$$

where $z = \frac{\pi x}{a}, T = \frac{\pi^2}{a^2}, a = \frac{E}{T}$ and $2q = \frac{V_o}{T}$

Eq. (4.2) is the Mathieu equation and its solution is derived for free electron or empty potential ( q ~ 0) when the crystal potential is flat as shown in Fig. (4.1). To determine the initial state wavefunction $\psi_i(x)$ in Eq. (4.2), we have included a surface of width ( $d$) in the crystal potential. The initial state wavefunction for the bulk and surface and for the vacuum regions is given by

$$\psi_i(x,q) = \begin{cases} (\frac{1}{4\pi k_i})^{\frac{1}{2}} \phi(x_0,q) e^{-\mu(x_o - x)} & x \leqslant 0 \\ (2\xi)^{\frac{1}{2}} e^{-\xi(x - x_o)} & x > 0 \end{cases} \qquad (4.3)$$

where $x_0$ = location of the crystal surface. In Eq. (4.3) above, we have $k_i = \sqrt{2E_i}$ and

$$\phi(x_0,q) = \lambda \cos m'x - \sin m'x,$$
$$\lambda = \tan m'(x_0 - \xi^{-1}). \qquad (4.4)$$

such that $m' = \frac{m\pi}{a}$, $m$ being the band gap index, $\xi$ is the height of step potential and $\lambda$ is the hybridization parameter.

Using the final state wavefunction $\psi_f$ as the scattering state of the step potential at x = 0, the photocurrent density is calculated by using the Fermi golden rule formula as

$$\frac{dj(E)}{d\Omega} = \frac{2\pi}{\hbar}\Sigma |<\psi_f|H'|\psi_i>|^2 \delta(E-E_f)\delta(E_f-E_i-\hbar\omega) f_o(E-\hbar\omega)[1-f_o(E)] \tag{4.5}$$

Here the perturbation is given by

$$H' = \frac{e}{2m_e c}(\boldsymbol{p}.\boldsymbol{A}+\boldsymbol{A}.\boldsymbol{p}) \tag{4.6}$$

and in one dimension, $H'$ can be written as

$$H' = \frac{e}{mc}[\tilde{A}_\omega(x)\frac{d}{dx} + \frac{1}{2}\frac{d}{dx}\tilde{A}_\omega(x)]$$

To compute the photon field, we have used the simple model of Bagchi and Kar which has been used earlier also. With simple modification the photon field used in our calculation can be written as

$$\tilde{A}_\omega(\omega,x) = \begin{cases} A_1, & x<-d \\ \frac{A_1.\varepsilon(\omega).d}{[1-\varepsilon(\omega)]x+d}, & -d \leqslant x \leqslant 0 \\ A_1.\varepsilon(\omega), & x>0 \end{cases} \tag{4.7}$$

where $A_1$ is a constant depending on the dielectric function $\varepsilon(\omega)$, photon energy $\hbar\omega$ and angle of incidence $\theta_i$. We have chosen $x_0 = \frac{a}{2}, \xi = \frac{12}{a}$ and $m = 1$. The reason

for the choice of m = 1 is that the surface state exists in the band gap for finite potential case. The matrix element in Eq. (4.5) can be written as the following for calculating the photocurrent :

$$I = \int_{-\infty}^{-d} \psi_f^* \tilde{A}_\omega(x) \frac{d\psi_i}{dx} dx + \int_{-d}^{0} \psi_f^* \tilde{A}_\omega \frac{d\psi_i}{dx} dx$$

$$+\frac{1}{2} \int_{-d}^{0} \psi_f^* \frac{d\tilde{A}_\omega(x)}{dx} \psi_i dx + \int_{0}^{\infty} \psi_f^* \tilde{A}_\omega(z) \frac{d\psi_i}{dx} dx. \qquad (4.8)$$

Photocurrent was calculated as a function of photon energy ($\hbar\omega$) by evaluating the integrals in Eq. (4.8). The formalism was then applied to the case of metals aluminium and beryllium as they are free electron type of metals. We see from the variation of photocurrent data that even in the case of Al and Be, it showed the qualitative behaviour as seen earlier in the theoretical and experimental data. The features seen in the behaviour of photocurrent in Al and Be can be attributed to the fact that in the free electron metals the change in bulk potential is too weak to impart sufficient momentum for photoexcitation. The surface photo-effect is due to the rapid variation of photon field in the surface region. This is evident from the matrix element in Eq. (4.5) where $d\tilde{A}_\omega/dx$ is directly dependent on photocurrent as the photon energy passes through the threshold for plasmon excitation. Moreover, we have considered a low photon energy photoemission, hence the incident radiation is too weak to photoexcite electrons from the bulk bands. The origin of peak in photocurrent data in the case of Be for $\hbar\omega < \hbar\omega_p$ has been explained by Karlsson *et. al.* from band picture. He attributed this to the existence of surface state at $\bar{\Gamma}$ with energy 2.8 eV in the bulk energy band gap $\Gamma_3^+ - \Gamma_4^-$.

## 4.2 **Strong Periodic Potential with Finite Surface** :

The case of empty lattice potential is not applicable to the strongly bonded metals like d-band metals or semiconductors. Hence one needs to develop the intial statre wavefunctions by solving the Mathieu equation in Eq. (4.2) by incorporating the sine and cosine elliptic functions. We have considered the same model as in the case of empty lattice potential model , but used for strong periodic lattice ( i.e. q > 0 ).

It is therefore, necessary to find an explicit form for $\phi(x'_0,q)$ in Eq. (4.3) to derive the intial state wavefunction $\psi_i(x)$. The most general form is a linear combination of all the bulk standing states $se_m(x'_0,q)$ and $ce_m(x'_0,q)$ for all the Fermi energy gap $m$ . Thus the surface states will be largely a hybrid of sine and cosine elliptic functions which is given by

$$\phi(x'_0,q) = \lambda_m ce_m(x'_0,q) - se_m(x'_0,q) \tag{4.9}$$

where $\lambda_m$ is the hybridization parameter which can be written as

$$\lambda_m = \frac{se_m(x'_0,q) - (\xi+\mu)^{-1} se'_m(x'_0,q)}{ce_m(x'_0,q) - (\xi+\mu)^{-1} ce_m(x'_0,q)} \tag{4.10}$$

Here $se_m(x'_0,q)$ and $ce_m(x'_0,q)$ are the sine and cosine elliptic functions in Eq. (4.9). These functions in expanded form can be written as

$$se_m(x'_0,q) = \sin mx'_0 - \frac{q}{4}\left[\frac{\sin(m+2)x'_0}{m+1} - \frac{\sin(m-2)x'_o}{m-1}\right] + \frac{q2}{32}\left[\frac{\sin(m+4)x'_o}{(m+1)(m+2)} + \frac{\sin(m-4)x'_o}{(m-1)(m-2)}\right] + .... \tag{4.11}$$

and $$ce_m(x'_0,q) = \cos mx'_0 - \frac{q}{4}\left[\frac{\cos(m+2)x'_0}{m+1} - \frac{\cos(m-2)x'_o}{m-1}\right]$$

$$+\frac{q2}{32}\left[\frac{\cos(m+4)x'_o}{(m+1)(m+2)} + \frac{\cos(m-4)x'_o}{(m-1)(m-2)}\right] + .... \qquad (4.12)$$

For finite surface potential, surface state existence condition implies that

$$x'_0 = x_0\tfrac{a}{2},\ \xi = \tfrac{12}{a},\ \lambda > 0 \text{ and } m = 3,5,.. \qquad (4.13)$$

We are considering surface state occuring for m = 3 and hence from Eqs. (4.11), (4.12) and (4.13), we can write,

$$ce_3(x'_o,q) = 0\ , \qquad ce'_3(x'_o,q) = 3(1+\frac{q}{16}-\frac{q^2}{640})$$
$$se_3(x'_o,q) = -1+\frac{q}{16}-\frac{11}{640}q^2\ , \qquad se_3(x'_o,q) = 0 \qquad (4.14)$$

Hence, we may obtain the value of $\lambda_3$ as :

$$\lambda_3 = \frac{(\xi+\mu)\left[1-\frac{q}{16}+\frac{11}{640}q^2\right]}{3(1+\frac{q}{16}-\frac{q^2}{640})} \qquad (4.15)$$

Using Eqs. (4.13) and (4.14) into Eq. (4.9), the intial state wavefuntion in the case of strong periodic potential becomes

$$\psi_i(x,q) = \begin{cases} (\frac{1}{4\pi k_i})^{\frac{1}{2}}(-1+\frac{q}{16}-\frac{11}{640}q^2)e^{-\mu(x'_o-x)} & x \leqslant 0 \\ (\frac{1}{4\pi k_i})^{\frac{1}{2}}e^{-\xi(x-x'_o)} & x > 0 \end{cases} \qquad (4.16)$$

The final state wavefunction $\psi_f$ as the scattering state of the step potential and photon field vector of Eq. (4.7) is used for computing the photocurrent by evaluating the matrix element in Eq. (4.8). Photocurrent was calculated as a function of photon energy ($\hbar\omega$) in the case of d-band metals like molydenum, tungsten, copper and semiconductor silicon. For each of these metals, the experimentally determined dielectric function were used for calculating the photon fields but the same surface parameters were used for all of these solids as it is a model calculation. The photocurrent data showed the experimental behaviour in photocurrent as measureed by Weng *et. al.* But the only difference in their case was that the photocurrent decreased to minimum at the plasmon energy. The plasmon energies for W and Mo are 25.3 eV and 24.4 eV respectively. For a narrow surface width( d = 0 ), the behaviour of photocurrent is completely different. We did not find any prominent peak for the values of photon energy below and above 15 eV photon energy.

It has been reported by Himpsel and Ortega that for Cu(100), Fermi level photoemission intensity when plotted as a function of photon energy, the data showed maxima at $\hbar\omega$ = 10.5 eV. Similar reports were also given by Eastman *et. al.* but with maximum intensity occuring at $\hbar\omega$ = 10.6 eV. In our case, our model calculations has shown peak in photocurrent at $\hbar\omega$ = 10 eV. The occurence of such peak in photocurrent in the band structure had been attributed to transition energy between the lower and upper s-p branch either at Fermi level or near it and has $\Delta_5$ symmetry. The case of photocurent for narrow surface width just produced a linear line of very negligible magnitude in photocurrent. We find that Cu has shown atleast the qualitative feature with the behaviour of photocurrent as indicated also by other metals like Pd, W, Si, etc. which were calculated earlier.

We also have calculated the wavefunction given in Eq. (4.16) to see whether this can reproduce the results calculated in the case of empty potential (q ~ 0) and for surface state condition m = 1. This was then applied to the case of Al and Be. It was seen that the photocurrent data was exactly the same as reported earlier both for Al and Be respectivley, which was shown in Fig. (4.2). In our calculations, we have included the case of narrow surface width. The reason for inclusion of narrow surface width is that it considers the Fresnel type of electromagnetic field. In Fresnel optics, the spatial variation of the photon field is not taken into consideration.

A study of these cases show that one can also make use of Mathieu type of potential in photoemission calculations. Though the model used is very simple, however, the inclusion of initial state wavefunction into the matrix element appears to produce the qualitative features as observed earlier in the experimentally measured data of photocurrent. The main drawback of the model used is that the same initial state wavefunction $\psi_i$ is used to describe both the surface and bulk regions of the solids under study. Also, we have used the same initial state energy for all the cases and also keeping constant the other parameters as it is a model calculation. However, it is interesting to note that the wavefunctions formulated for strong periodic potential easily reproduces the wavefunctions for empty potential(free electron) cases. It would be further interesting to extend such type of model to include the band structure effects in the electronic structure calculations.